IAC–18–C1.9.5

Mars Optimal Aerobrake Maneuver Estimation

Bruno V. Sarli
NASA/GSFC Science Collaborator, Catholic University of America, bruno.victorinosarli@nasa.gov

Ariadna Farres
NASA/GSFC Science Collaborator, University of Maryland Baltimore County, ariadna.farresbasiana@nasa.gov

David C. Folta
Aerospace Engineer, NASA Goddard Space Flight Center, david.c.folta@nasa.gov

Abstract

Mars science satellites often perform orbit changes to obtain different measurements, ground tracks or relay operations. Large reductions in semi-major axis and eccentricity can be done efficiently using the atmospheric drag, a.k.a aerobrake. Aerobraking is one of the most challenging planetary orbit maneuvers in terms of planning and operations. The most important consideration for aerobraking is maintaining the spacecraft's periapsis within an allocated atmospheric density corridor, which is accomplished by raising or lowering periapsis through one or a series of very small and short maneuvers. These maneuvers must be performed as efficiently as possible due to propellant constraints. Work herein details a fast and accurate method to calculate the required impulsive velocity changes in the orbit to guarantee that the spacecraft remains in a prescribed density corridor. The method makes use of the orbit's state transition matrix to map the solution space around the reference orbit. It evaluates the most efficient maneuver epochs to target a given periapsis change with a linear optimal control for single or multiple maneuvers. A fast calculation of the maneuver allows for a more comprehensive evaluation of the trade space, and the selected maneuver may be re-targeted later with a higher-fidelity model. Comparisons against fully propagated models and direct method optimizations demonstrate the new method's performance.

1. Introduction

Aerobraking is the process of using high atmospheric drag, together with maneuvers made by an attitude control system, to change a spacecraft's orbit.[1] Generally, the atmospheric brake is used to decrease apoapsis without relying exclusively on propellant. However, chemical maneuvers are necessary to keep the spacecraft in an allowed density atmospheric corridor, in which the changes to the orbit are acceptable. The chemical maneuvers are short enough and small enough that they may be considered impulsive. Due to the ever diminishing quantity of propellant remaining in the spacecraft, the maneuvers need to be as efficient as possible in order to maximize the mission's operational lifetime. Another important factor for the evaluation of an aerobrake scheme is the planetary environment through which the spacecraft will go, which defines the density profile. Particularly, Mars is the focus of this study. Several factors affect the Martian atmospheric density, which has a complex evolution with variations coming from Solar cycles, Martian albedo and seasons, as well as atmospheric winds and dust storms. The range that defines the mission's density corridor incorporate factors such as maximum structural acceleration given by the drag force acting on the vehicle, and the velocity changes that would result in an orbit escape or entry.

Aerobrake maneuver schemes are challenging for many reasons. Perhaps the most important from a flight dynamics perspective is the need to accurately account for orbital perturbations. Particularly for Martian missions, higher-order gravitational perturbations, perturbing gravitating third bodies and atmospheric drag must all be accounted for in order to accurately predict the evolution of the spacecraft's orbit. Moreover, the inclusion of drag effects requires consideration of the spacecraft's attitude and the dynamics of the Martian atmosphere, which adds considerable complexity to the problem's modeling.

A method to calculate an optimal aerobrake ma-

neuver scheme that minimizes the propellant consumption is the main goal of this study. Herein, the impulsive maneuvers are targeted to keep the orbit's periapsis within the defined density corridor. The proposed method uses the spacecraft orbit's state transition matrix (STM), propagated with several perturbation models, to evaluate the stability of the spacecraft's final position with respect to the velocity throughout the trajectory. The most unstable points within the trajectory define the most efficient maneuver timings to change the final position; however, these points may not necessarily be in the desired direction (periapsis in this case). Nevertheless, this region of the orbit is generally known for most cases because perturbations are small and corrections frequent - making the orbit quasi-Keplerian within these regions. For maneuvers that raise or lower the periapsis, as is the case for aerobrake, these multiple revolution orbits with small second-order perturbations will have the most efficient maneuver point at or very near the apoapsis. Once the number and time of the impulses are defined, a linear optimal control policy is derived using the STM.[2] This strategy defines the optimal direction and magnitude of each impulse to target the desired orbital parameters.

The Mars Atmosphere and Volatile EvolutioN (MAVEN) mission, currently in orbit around Mars, is used here as an example for the method's application.[3] The spacecraft routinely performs deep dives in the Martian atmosphere to gather atmospheric science data, making it a suitable test case.

Section 2 details the aerobrake scheme, including the dynamic model used in this paper. Section 3 describes the method used in this work, detailing the mathematics behind it. An example of the mission's aerobrake scenario is shown in Section 4.

2. Problem Modeling

Aerobrake analysis primarily involves maneuver design and operational verification. This analysis is currently centered on the use of high-fidelity propagators employed for all mission maneuvers. These are typically slow in computing a single solution and are not suitable for large scale trade studies or large Monte Carlo runs. The method developed in this study aims to improve the computational speed in analyses that trade multiple solutions as a first understanding of the scenario which informs the high-fidelity tools. In addition, it helps to establish orbit designs and procedures for the mission's aerobrake support models. It is, however, important to comply with high-fidelity operational modeling for accuracy with a fast computation time. The goal is to allow the analysis of numerous aerobrake maneuver plans to minimize the propellant usage and provide various operational scenarios, such as to be proactive and permit quick assessment of aerobrake maintenance options, contingencies, variations in maneuver plans, minimal maneuvers, maneuver timing, multiple maneuvers, etc.

To model the dynamics of a satellite around Mars, it is necessary to consider the main forces affecting its motion. In this paper, the following are considered: (a) the gravity field of Mars using the Mars-50C harmonics up to degree and order 50;[4] (b) the atmospheric drag using Mars GRAM-2005;[5] (c) the solar radiation pressure (SRP) using the cannonball model (spacecraft's attitude evaluation is out of the scope of this work); and, (d) the point mass gravity perturbations from the Sun, Jupiter, Phobos and Deimos. State propagation is performed using the General Mission Analysis Tool (GMAT).[6] GMAT is an open-source tool for space mission design and navigation that has been developed at NASA Goddard Space Flight Center. The tool enables trajectory optimization and mission design regimes ranging from low Earth orbit to lunar applications, interplanetary trajectories and other deep space missions. Two of this tool's capabilities are of particular interest here: easy, flexible computation of trajectories around Mars using high-fidelity force models and the ability to generate the STM through the propagation of the variational equations.[7] This propagation of the STM using a high-fidelity model allows for mapping the region around a reference orbit with a good representation of the second-order effects already described above. While this study uses GMAT, the methodology presented in this paper is independent of the force-model and numerical integration tools. As long as the reference orbit and the STM are provided, the methodology presented here can be applied.

3. Aerobrake and Maneuver Models

The aerobrake analysis proposed here combines the computation of a reference orbit and a high-fidelity propagated STM associated with this orbit. These are used in a targeting scheme that is able to minimize the propellant with single or multiple maneuvers. In this section, different parts of the methodology are presented.

3.1 Problem Base Formulation

To fix notation, let $\dot{\mathbf{x}} = f(t, \mathbf{x})$ be the equations of motion for the force model, where $\mathbf{x} = [\mathbf{r}, \mathbf{v}]$ is

a 6×1 vector. In order to compute the trajectory and its associated STM from the force model's Jacobian matrix, it is necessary to integrate the extended system:

$$\begin{array}{rcll} \dot{\mathbf{x}}(t) & = & f(t, \mathbf{x}(t)), & \mathbf{x}(t_0) = \mathbf{x}_0, \\ \dot{\Phi}(t) & = & A\Phi(t), & \Phi(t_0) = I_{6\times 6}, \end{array} \quad [1]$$

where t_0 is the initial epoch, $\mathbf{x}_0$ is the initial state, $A = Df_{\mathbf{x}}$ is the Jacobian of the force model and $I_{6\times 6}$ is the 6×6 identity matrix.

Let $\varphi_t(t_0, \mathbf{x}_0)$ be the flow associated to the equations of motion[8] (i.e. the solution at time t for an initial condition $t = t_0$ and $\mathbf{x} = \mathbf{x}_0$). For simplicity, $\varphi_0(t) = \varphi_t(t_0, \mathbf{x}_0)$.

The satellite states at final epoch t_f are given by $\varphi_0(t_f)$ and the associated STM by $\Phi(t_f, t_0) = \Phi(t_f, (t_0, \mathbf{x}_0))$. If $\mathbf{x}_1$ is an initial condition close to $\mathbf{x}_0$, a first-order Taylor approximation can be made:

$$\varphi_1(t_f) \approx \varphi_0(t_f) + \Phi(t_f, t_0)(\mathbf{x}_1 - \mathbf{x}_0), \quad [2]$$

where $\varphi_1(t_f)$ represents the spacecraft's states at $t = t_f$ starting at $t = t_0$ and $\mathbf{x} = \mathbf{x}_1$. This equation maps first-order variations in the initial state to the state at t_f. In this study, this equation is used to map the effects of $\Delta\mathbf{v}$ maneuvers.

3.2 Single Impulsive Maneuver

As mentioned previously, an aerobraking spacecraft's periapsis needs to be kept within a given density corridor due to operational, thermal and structural constraints to take advantage of the atmospheric drag to lower its apoapsis without putting the vehicle at risk. Therefore, each time the satellite moves out of this corridor, or is about to, a Δv maneuver is performed to raise or lower the periapsis, placing it back inside the allowed density range. Precomputing a reference orbit and its STM facilitates a fast calculation of these various possible $\Delta\mathbf{v}$'s, allowing a trade study between the propellant cost and maneuver epoch.

Let $\delta\mathbf{x}_f = \varphi_1(t_f) - \varphi_0(t_f)$ be the final displacement between two orbits and $\delta\mathbf{x}_i = \varphi_1(t_i) - \varphi_0(t_i)$ its initial difference. Equation 2 can be rewritten as

$$\delta\mathbf{x}_f = \Phi(t_f, t_i)\delta\mathbf{x}_i, \quad [3]$$

where $\delta\mathbf{x}_i^T = (\emptyset_{1\times 3}, \Delta\mathbf{v}^T)$ and $\delta\mathbf{x}_f^T = (\delta\mathbf{r}_f^T, \delta\mathbf{v}_f^T)$. The solution of Eq. 3 results in the required $\Delta\mathbf{v}$ to change the spacecraft's final states. Given that the only constraint imposed is a change in the orbit radius, $\delta\mathbf{r}_f$, this simplifies the problem to solving a 3×3 linear system:

$$\Delta\mathbf{v} = \Phi_{RV}^{-1}\delta\mathbf{r}_f, \quad [4]$$

where

$$\Phi(t_f, t_i) = \begin{bmatrix} \Phi_{RR} & \Phi_{RV} \\ \Phi_{VR} & \Phi_{VV} \end{bmatrix}. \quad [5]$$

Hence, having computed the STM throughout a full trajectory, a quick analysis can be done by solving Eq. 4 for the different points in the trajectory. This provides a relation between the maneuver epoch and the $||\Delta\mathbf{v}||$ cost for a given change in the final position, $\delta\mathbf{r}_f$.

3.3 Multiple Impulsive Maneuvers

In order to analyze multiple maneuvers along the trajectory, a similar approach as before can be derived. Given a set of epochs along the reference trajectory, $\{t_1, \ldots, t_n\}$, where the maneuvers are to be placed (Fig. 1), an optimal multiple maneuver scheme can be derived utilizing the linear regime mapped by the STM.[2]

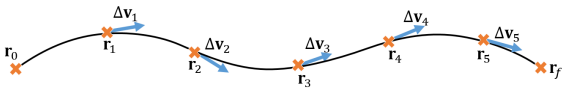

Fig. 1: Multiple-impulse maneuver scheme

Let $\delta\mathbf{x}_f^T = \left[\delta\mathbf{r}_f^T, \delta\mathbf{v}_f^T\right]$ be the final deviation from the reference orbit at periapsis. If $\{\Delta\mathbf{v}_1, \ldots, \Delta\mathbf{v}_n\}$ is a set of maneuvers applied at epochs $\{t_1, \ldots, t_n\}$, a linear approximation of the final deviation from the reference orbit can be calculated as:

$$\begin{array}{rcl} \begin{bmatrix} \delta\mathbf{r}_f \\ \delta\mathbf{v}_f \end{bmatrix} & = & \Phi(t_f, t_n) \begin{bmatrix} \emptyset_{3\times 1} \\ \Delta\mathbf{v}_n \end{bmatrix} + \\ & + \cdots + & \Phi(t_f, t_1) \begin{bmatrix} \emptyset_{3\times 1} \\ \Delta\mathbf{v}_1 \end{bmatrix}. \end{array} \quad [6]$$

As the only condition imposed is a final position state change, $\delta\mathbf{r}_f$, the above equation can be expressed as:

$$\delta\mathbf{r}_f = \left[\Phi_{RV}(t_f, t_n) \cdots \Phi_{RV}(t_f, t_1)\right] \begin{bmatrix} \Delta\mathbf{v}_n \\ \vdots \\ \Delta\mathbf{v}_1 \end{bmatrix}. \quad [7]$$

The under-determined linear system (more unknowns than equations, has no unique solution) given by Eq. 7 can be solved by finding the solution that minimizes a certain cost function. For simplicity, this equation can be expressed as

$$\delta\mathbf{r}_f = \bar{\Phi}\Delta\bar{\mathbf{v}} \rightarrow \delta\mathbf{r}_f - \bar{\Phi}\Delta\bar{\mathbf{v}} = 0, \quad [8]$$

and used to augment the cost function representing the square magnitude of control,

$$J = \frac{1}{2}\sum_{i=1}^{n} \|\Delta \mathbf{v}_i\|^2 . \quad [9]$$

To find the solution of Eq. 8 that minimizes Eq. 9, it is necessary to find the extremals of the functional:

$$\bar{J} = \frac{1}{2}\Delta\bar{\mathbf{v}}^T \Delta\bar{\mathbf{v}} + \lambda^T \left(\delta\mathbf{r}_f - \bar{\Phi}\Delta\bar{\mathbf{v}}\right). \quad [10]$$

Following reference,[2] the solution that minimizes the above equation satisfies,

$$\Delta\bar{\mathbf{v}} = \bar{\Phi}^t \left(\bar{\Phi}\bar{\Phi}^t\right)^{-1} \delta\mathbf{r}_f. \quad [11]$$

Equation 11 can be evaluated for various sets of epochs in order to compare different scenarios for n impulsive maneuvers with their the total $\Delta\mathbf{v}$ cost. Therefore, to find the set of $\Delta\bar{\mathbf{v}} = [\Delta\mathbf{v}_1, \ldots, \Delta\mathbf{v}_n]$ resulting for each set of epochs $\{t_1, \ldots, t_n\}$ it is only necessary to evaluate Eq. 11, which can be done efficiently. There is no integration required to solve this system as the STM has been precomputed before the trade analysis is performed, allowing great flexibility comparing different maneuver options in an efficient way.

3.4 Periapsis Poincaré Map

In the two previous sections, the linear approximation of the flow (i.e., the STM) was used to find the required $\Delta\mathbf{v}$ for a given final position displacement. Recall that the STM measures the orbital displacement in time, but it does not guarantee the final position is a periapsis. In fact, after the maneuver is performed, the orbit period changes and the final point will, most likely, no longer be the periapsis. The exception would be if the point being targeted coincides with the periapsis after the maneuver; such conditions can only be found after the maneuver is calculated. Therefore, further constraints need to be applied in order to guarantee that the desired change is in fact at the periapsis after the maneuver. For this goal, the periapsis Poincaré map is introduced.

Let $P(t, \mathbf{x}) = \varphi_{T(\mathbf{x})}(t, \mathbf{x})$ be the periapsis-map, i.e. a map that takes an initial state $(t_0, \mathbf{x}_0)$ to the final state $\mathbf{x}_f = P(t_0, \mathbf{x}_0)$ such that $\mathbf{x}_f$ is a periapsis with $T(x_0)$ being the time required to reach it. A point $\mathbf{x} = (\mathbf{r}, \mathbf{v})$ along an orbit is a periapsis if it satisfies:

$$\{(\mathbf{r}, \mathbf{v}) \mid \langle \mathbf{r}, \mathbf{v}\rangle = 0, \langle \dot{\mathbf{r}}, \dot{\mathbf{v}}\rangle \geq 0\}.$$

The Poincaré map $P(t, \mathbf{x})$ and its differential $DP_{\mathbf{x}}$ can be computed numerically: $P(t, \mathbf{x})$ by integrating the trajectory until the desired periapsis is reached; and $DP_{\mathbf{x}}$ by performing a simple correction to the classical STM:

$$DP_{\mathbf{x}}(x) = -f(P(x))DT(x) + D\varphi_{T(x)}(x), \quad [12]$$

$$DT(x) = \frac{Dg(P(x))D\varphi_{T(x)}(x)}{Dg(P(x))f(P(x))}, \quad [13]$$

where $DT(x)$ is the time derivative to reach the Poincaré section, $P(x)$ represents the image of the periapsis Poincaré map $P(t, \mathbf{x})$, $D\varphi_{T(x)}(x)$ is the STM for $\mathbf{x}$ at the time it reaches periapsis, $f(x)$ is the equation representing the force model ($\dot{\mathbf{x}} = f(x)$) and $g(x) = \langle \mathbf{r}, \mathbf{v}\rangle$ is the equation representing the surface of section with Dg representing its derivative.

As in Eq. 2, the first-order approximation of the points in the periapsis-map is given by:

$$P(\mathbf{x}_1) \approx P(\mathbf{x}_0) + DP_{\mathbf{x}}(\mathbf{x}_0)(\mathbf{x}_1 - \mathbf{x}_0). \quad [14]$$

Hence, to find the $\Delta\mathbf{v}$ that will change the position of the periapsis by $\delta\mathbf{r}_f$, it is necessary to solve the linear system:

$$\delta\mathbf{r}_f = \Pi_{RV}\Delta\mathbf{v}, \quad [15]$$

where

$$DP_{\mathbf{x}}(x) = \begin{bmatrix} \Pi_{RR} & \Pi_{RV} \\ \Pi_{VR} & \Pi_{VV} \end{bmatrix}. \quad [16]$$

Using Π_{RV} in Eqs. 4 and 11 instead of Φ_{RV} ensures that the $\Delta\mathbf{v}$'s found change the position of the final periapsis by $\delta\mathbf{r}_f$ and that $\mathbf{r}_{new} = \mathbf{r}_f + \delta\mathbf{r}_f$ is also a periapsis.

3.5 Periapsis Targeting

In Sections 3.2 and 3.3, a new approach on how to find a $\Delta\mathbf{v}$ to change the final periapsis by $\delta\mathbf{r}_f$ was discussed. This can be done by simply solving a linear system (Eq. 4 and Eq. 11).

The constraint for aerobraking is to keep the periapsis at a certain density corridor, hence a range of periapsis altitudes. As the density profile with, for example, Mars GRAM-2005 is mapped around the planet's coordinates, the periapsis altitude at a particular epoch can always be related to the density. However, the procedure described above solves a linear system to target a specific new periapsis location. In order to find the optimal maneuver, it is needed to define a set of periapsis locations at the same altitude, and find the maneuver with minimum Δv. A gradient based search method is applied to find this minimum (SNOPT[11] is used here).

The periapsis change is parameterized using spherical coordinates: two angles (α, β) and an altitude (R_p):

$$\delta\mathbf{r}_f(R_p,\alpha,\beta) = R_p\left(\cos\beta\cos\alpha\ \hat{\mathbf{r}} + \cos\beta\sin\alpha\ \hat{\mathbf{v}} + \sin\beta\ \hat{\mathbf{h}}\right) - \mathbf{r}_f, \quad [17]$$

where $\mathbf{r}_f$ is the periapsis vector with $\hat{\mathbf{r}} = \mathbf{r}_p/||\mathbf{r}_p||$ being its direction, $\hat{\mathbf{v}} = \mathbf{v}_p/||\mathbf{v}_p||$ is the periapsis normalized velocity, and $\hat{\mathbf{h}} = \mathbf{r}_p\times\mathbf{v}_p/||\mathbf{r}_p\times\mathbf{v}_p||$ completes the right-handed set of coordinate axes, Fig. 2.

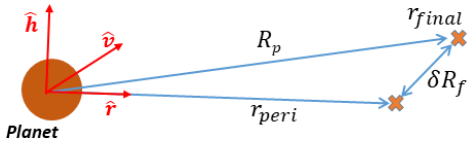

Fig. 2: Periapsis target

Notice that for a given α, β, if Π_{RV} has full rank, there exists a unique $\Delta\mathbf{v}$ that satisfies Eq. 4 in the case of a single impulse maneuver, and Eq. 11 in the case of multiple maneuvers. Then SNOPT will find the optimal solution α^*, β^* that satisfies Eq. 4 or Eq. 11 (depending on the case) and minimizes $||\Delta\mathbf{v}||^2$. Not fixing the final periapsis location and letting the optimizer find it enables the tool to locate the optimal transfer; accounting for all the secondary effects that alter the orbital parameters.

As an example, an elliptic orbit around Mars is considered, whose orbital parameters are summarized in Tab. 1. The reference orbit and its STM have been computed up to the periapsis passage that happens 14 days after the starting point. For each point along the orbit, the required $\Delta\mathbf{v}$ (single maneuver) necessary to raise the final periapsis back to its initial altitude is computed; for this example a 5.65 km raise is required.

The top plot in Fig. 3 shows the altitude change over time for the first 2 days. The bottom plot shows the evolution of the $||\Delta\mathbf{v}||$ required to raise the periapsis: unconstrained location (min. $||\Delta\mathbf{v}||$) in red and along $\hat{\mathbf{r}}$ (i.e $\alpha = 0$, $\beta = 0$ on Eq. 17) in blue. Notice how the minimum $||\Delta\mathbf{v}||$ correspond to performing the maneuver at apoapsis. Moreover, a change along the same line of the periapsis can result in large maneuvers. In order to illustrate this, Fig. 4 shows the surface sections of $||\Delta\mathbf{v}||$ as a function of the angles α, $\beta \in [-2.5°, 2.5°]$ in Eq. 17, at four different locations along the orbit (highlighted with a black dot on the top plot of Fig. 3). Close to the apoapsis (in plot, points a and b), the location of the minimum $||\Delta\mathbf{v}||$ is close to $\alpha = \beta = 0$, while in other cases (in plot, points c and d), the location of this minimum is slightly displaced. Moreover, looking at b and d, the slope of the function is very steep, resulting on large $||\Delta\mathbf{v}||$ for small changes on the target periapsis.

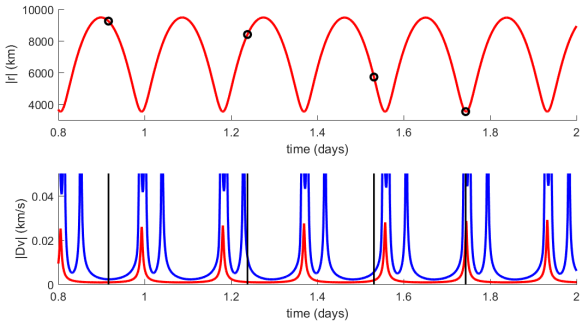

Fig. 3: Top: Distance to Mars over time. Bottom: Δv cost of maneuver over time.

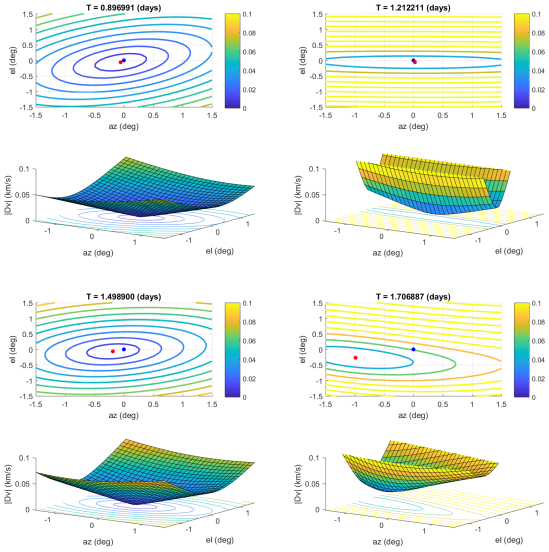

Fig. 4: Contour levels of the required $||\Delta\mathbf{v}||$ to raise periapsis as a function of the angles α, β.

3.6 Event Epoch Correction

Recall that when solving for multiple impulsive maneuvers, after the first maneuver, the time of passage by the apses is shifted. Because these shifts are very small, the linear approximation to do the full analysis still holds. Nevertheless, when simulating

the sequence of maneuvers, the apoapsis epoch has to be changed, as illustrated in Fig. 5.

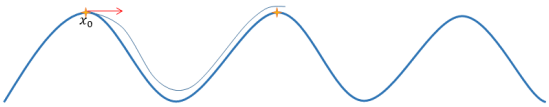

Fig. 5: Orbit change due to maneuver

Using the same formulation as for the peripasis-map (Section 3.4), the apoapsis-map can be defined and a first-order approximation of the new time of passage by apses can be numerically estimated. Let $T_a(\mathbf{x}_i)$ be the apsis epoch for a state $\mathbf{x}_i = (\mathbf{r}_i, \mathbf{v}_i)$. When a $\Delta\mathbf{v}$ maneuver is performed, $T_a(\mathbf{x}_0 + \mathbf{h})$ is the new apsis epoch where $\mathbf{h} = (0, \Delta\mathbf{v})$. Equation 13 can estimate, up to first order, the new apsis epoch: $T_a(\mathbf{x}_0 + \mathbf{h}) = T_a(\mathbf{x}_0) + DT_a(\mathbf{x}_0)\mathbf{h}$.

4. Method Evaluation

As an example of aerobrake design and the tool usage, the MAVEN mission is selected because it is currently an operational mission that regularly performs atmospheric deep dips. MAVEN was designed to determine the role that loss of volatiles from the Mars atmosphere to space has played through time, giving insight into the history of Mars' atmosphere and climate, liquid water, and planetary habitability.[9] To the current date, the MAVEN spacecraft has been orbiting Mars for four years in a highly-inclined and highly-elliptic orbit.[10] As part of the proposed extended relay mission, an apoapsis decrease is required to place the spacecraft in a safe stable orbit (lower orbits are more efficient for relay operations).

Fig. 6 shows the spacecraft's orbit in a Mars J2000 equatorial reference frame propagated for approximately 14 days. The mission trajectory's epoch and orbital elements are given in Tab. 1. MAVEN is in quasi-Keplerian orbit, meaning that perturbations are small enough to render the orbit close to invariant. During aerobrake, changes are mainly at the apoapsis altitude, while the other orbital elements remain close to their original values during the 14 days under consideration.

A simple analysis of the eigenvalues associated with the second quadrant of the STM (Φ_{RV}) shows that the stability of the final position (in this case, periapsis) with respect to the velocity, $\frac{\partial \mathbf{r}_f}{\partial \mathbf{v}_i}$, degrades close to the apoapsis (see Fig. 7). Unstable regions mean that a change in velocity at this point will result in a greater change at the final position. However, a simple stability check does not guarantee the best point for an optimal maneuver at a specific angle nor the correct change in the periapsis direction. To find such conditions, a single maneuver change can be applied throughout the trajectory, analyzing the points with the lowest Δv requirements. As was shown in the previous sections, (e.g. Fig. 3), the or-

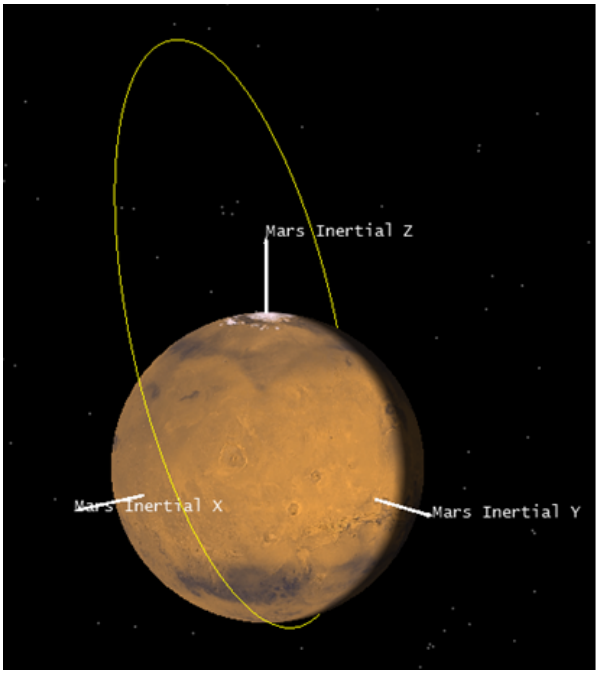

Fig. 6: MAVEN's propagated orbit

Table 1: MAVEN spacecraft's parameters

Epoch UTC	15 Oct 2017 15:50:00.000
Semi-major axis	6501.987 km
Eccentricity	0.459
Inclination	103.759°
Arg. of periapsis	0.339°
RAAN	9.553°
True anomaly	217.080°
Wet mass	757.00 kg
Drag coefficient (C_D)	2.20
Drag Area	26.54 m^2
SRP coefficient (C_R)	2.00
SRP Area	20.00 m^2

*Mars J2000 equatorial reference frame

bit's apoapsides are the most efficient points to apply the maneuvers.

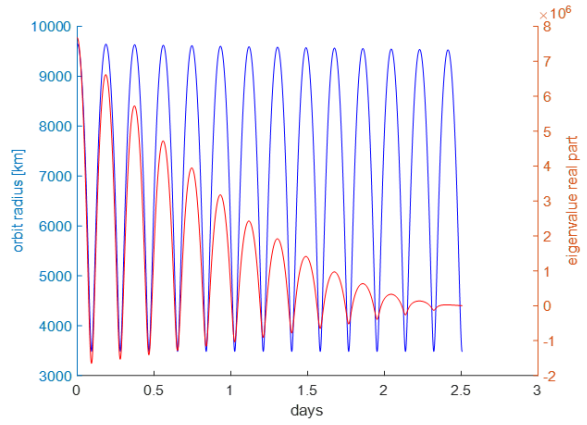

Fig. 7: Eigenvalues of $\frac{\partial \mathbf{r}_f}{\partial \mathbf{v}_i}$

The method developed here is used to generate different sets of solutions. For the comparison in this section, a more challenging result with four impulses is selected. The results are displayed in Fig. 8, with the lowest Δv selected having a total of 0.823 m/s for a periapsis raise of 5.6547 km. The characteristics of each individual impulse are shown in Tab. 2. Two comparisons are then performed: (a) same maneuvers at the same time propagated in high-fidelity; and (b) same maneuvers used as an initial guess for an optimization problem to minimize the use of propellant.

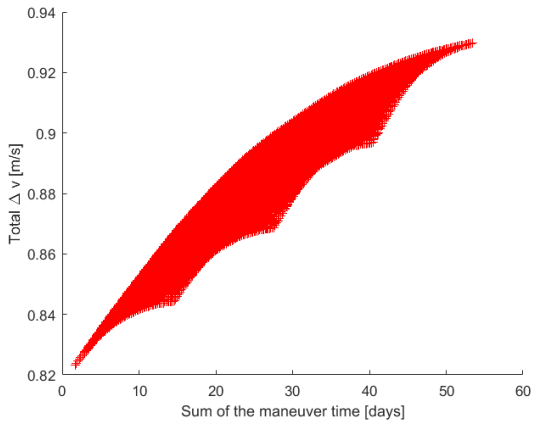

Fig. 8: Multiple impulse analysis

4.1 Hight-Fidelity Propagation Comparison

The first assessment of the method is in the accuracy of the solution. Recall that the linear approximation has been used to find a set of maneuvers to reach a specific periapsis. In this section, the best four-impulse solution described above is compared against the result of the same maneuvers at the same epochs propagated with a high-fidelity model. The maneuvers as well as their epochs from 15 Oct 2017 used in the propagation are outlined in Tab. 2.

Table 2: Maneuvers in high-fidelity

Epoch (s)	Δv_x (m/s)	Δv_y (m/s)	Δv_z (m/s)	$\|\Delta v_x\|$ (m/s)
12386	-7.441e-03	4.887e-02	-0.201	0.207
28310	-8.069e-03	4.849e-02	-0.200	0.206
44231	-8.561e-03	4.807e-02	-0.200	0.205
60154	-9.157e-03	4.760e-02	-0.199	0.205

The propagation result shows that the Δv calculated linearly can in fact reach 5.2973 km after 14 days, which, therefore, gives an error of 0.35645 km. A 6% error is considered reasonable given that the STM quality degrades over time, and, for operational purposes, 14 days is about double the amount of time that a maneuver operation would take place. Granted that it is not necessarily a linear relation between time and accuracy, a 7 days periapsis change (rather than 14 days) would have a considerably smaller error.

4.2 Optimization Comparison

In the second comparison, a direct method optimizer (DMO) is used to generate the solution given by the linear method. The gradient based optimizer used here is SNOPT, a sequential quadratic programming algorithm.[11]

The problem is set up as a plain single forward shooting problem that, though not the most efficient transcription, is enough to reach an optimal solution in a feasible amount of time to allow a comparison of the results. Table 3 shows the optimal solution calculated with the high-fidelity model, the linear method, and their differences. The optimization finished successfully with four major iterations and a maximum of four minor iterations and reached an optimality tolerance of 4.8×10^{-7} (normalized units).

Results outline that the linear method correctly calculated the maneuvers with 10^{-2} m/s accuracy. The gradient-based optimizer had difficulty in finding the maneuver epochs as it can be seen by the fact

Table 3: Comparison of direct method optimization and linear method solutions

	DMO	Linear	Difference
Δv_1 (m/s)	0.220	0.207	0.0137
Epoch (s)	12386.219	12386.219	0.0
Δv_2 (m/s)	0.219	0.206	0.0125
Epoch (s)	28310.328	28310.328	0.0
Δv_3 (m/s)	0.219	0.205	0.0136
Epoch (s)	44231.305	44231.305	0.0
Δv_4 (m/s)	0.218	0.205	0.013
Epoch (s)	60161.579	60153.524	8.052
Total Δv (m/s)	0.876	0.823	0.053
Periapsis (km)	3521.386	3521.389	2.461 m
Epoch (s)	1190515.179	1192750.252	37.251 min

that the epoch of the first three maneuvers are zero. This result particularly shows the importance of the method developed here to search and trade among the different maneuvers' epochs. It is worth noticing that this single optimization with DMO in high-fidelity took multiple hours, while a full set of linear solutions were calculated in less than 5 seconds.

5. Aerobrake Campaign Example

Earlier sections demonstrated how the method compares with the propagated solutions, which are generally how solutions are generated for missions. However, in this section, two tool usage tests are shown. First, a trade study is performed for a targeted change in the periapsis with up to four maneuvers, and considering all possible combinations of apoapsis for their epochs. Second, for a given set of maneuver epochs, an example explores how a change in the periapsis altitude affects later apoapsis decay. In this example, the maneuver's epochs can be selected by the trade study or a fixed given set of epochs (for example, the communication link periods).

5.1 Trade study

A set of solutions is generated for this orbit. The problem is set to raise the orbit's final periapsis by 5.6547 km using 1, 2, 3 or 4 maneuvers applied at the different apoapsides. It also includes the associated position error due to incorrect execution time and the Δv change required to correct for such error. Fig. 9 shows the aforementioned trade study on the number of impulsive maneuvers with the total Δv for each case in the y-axis and the sum of the execution epochs in the x-axis. A single maneuver at the very first apoapsis is the most efficient way to change the periapsis; however, it is also the most prone to errors as the entire chance is made at a single point. Four maneuvers, although slightly more expensive, allow the total error to be spread among all the points. In terms of operations, more maneuvers can potentially be more attractive as modeling or even execution errors can be later corrected by the subsequent Δv's given that orbit determination will be done in between maneuvers. Due to this, the cheapest four impulsive solution is selected for the following error analysis.

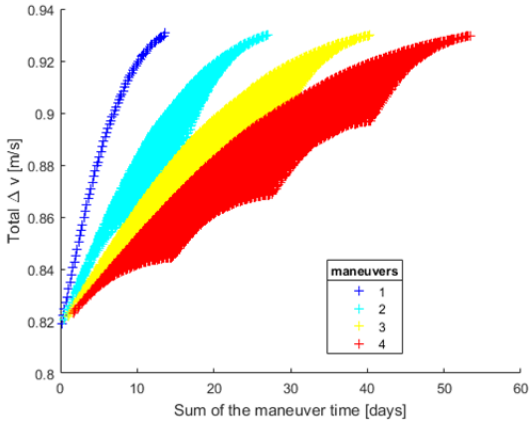

Fig. 9: Multiple impulse analysis

The position error due to an early or late maneuver execution, Fig. 10, shows, for example, a position error of up to 120 meters within a range of 200 seconds execution time error. If, on the other hand, the mission is aware that the delay will happen, the Δv required at the same time to reach the correct change in the periapsis, Fig. 11, varies on the order of millimeters per second for the 200-seconds range.

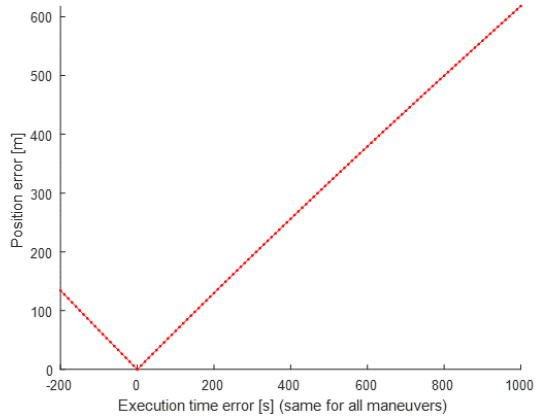

Fig. 10: Position error due to delayed execution time

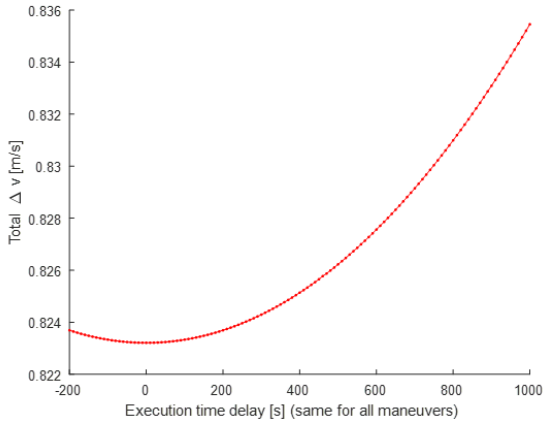

Fig. 11: The Δv correction due to delayed execution time

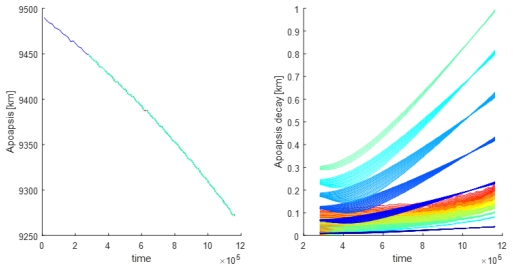

Fig. 12: Apoapsis decay from single Δv maneuver

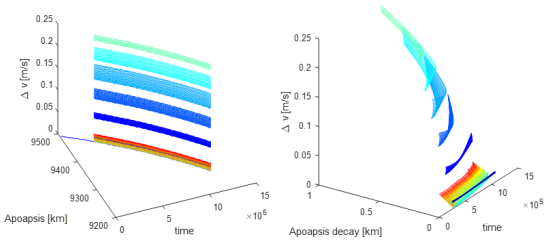

Fig. 13: Apoapsis decay from single Δv maneuver with magnitudes

5.2 Apoapsis Decay

Another important consideration for planning purposes is the rate at which apoapsis decays for different periapsis targets. After all, this is the main objective of an aerobrake. For this example, a single maneuver is selected to be executed in one of the apoapsides to raise the periapsis 3.269 days after the initial epoch. All the apoapsides before the targeted periapsis are included in the trade study. Eleven different δr's ranging from 0.1 km to 5.1 km with increments of 0.5 km are targeted starting at the different apoapsides. After the maneuver is performed and the periapsis is changed, the apoapsis evolution is calculated using the apoapsis-map STM.

Fig. 12 shows in the left plot the apoapsis decay with respect to the planet's surface; different colors indicate the result given by the different targeted points in the periapsis. The target points and the rate of decay are more clear on the right plot. In the right-hand plot each color, i.e. periapsis point, has several lines corresponding to the different Δv's used to target the point. These Δv requirements became more clear in Fig. 13, where a third axis is added in which the total Δv of each solution is outlined.

These plots outline the trade-off between decay rate and the required $||\Delta v||$ to reach a particular periapsis altitude. Note that the lower the periapsis is the higher the apoapsis decay rate is.

6. Conclusions

Aerobrake maneuvers require precision and fast turnaround for maneuver planning. The atmospheric brake is generally combined with small chemical maneuvers targeted to alter the periapsis to keep it within a given density range, which originates from mission constraints. This paper presents an alternative method to perform trade studies between maneuver executions to re-target the orbit periapsis, using only a reference orbit propagated on a high-fidelity model and its STM. The main advantage of using a reference orbit and its STM is that one can compute the required set of Δv's to change the periapsis altitude by simply solving a linear system facilitating fast solutions for large studies that would typically require long simulations with high-fidelity models.

Several tests are presented to check the fidelity of the results and the ability of the developed methodology to find optimal solutions. Results show an average of 0.081% error per orbit on the altitude prediction with an accumulated 6% error over 74 orbital revolutions, which is remarkable considering that the computations where done on a 14-day propagation.

Finally, an aerobrake campaign for MAVEN has been analyzed as an example to show the versatility of the approach. A trade study between 1, 2, 3, and 4 impulsive maneuvers was analyzed for a reference trajectory of 14 days around Mars. Apart from comparing the cost of changing the periapsis between the different cases, an analysis on the execution error is presented. Furthermore, the trade in the Δv and periapsis target that result in different apoapsis decay

rates is analyzed.

The method developed for this study has shown to reasonably predict the optimal aerobrake maneuvers (time, direction and magnitude) when compared to a direct optimization method with high-fidelity orbital perturbations. Its software implementation permits orders-magnitude faster calculation, allowing it to be used in large searches, such as grid and Monte Carlo.

Acknowledgments

This work has been supported by the NASA Goddard Space Flight Center's Space Science Mission Operations through the MAVEN mission. The researcher Bruno Sarli has been funded through the CREST program at the Catholic University of America under the task 690.008. The researcher Ariadna Farres has been funded through the Goddard Planetary Heliophysics Institute task 595.001 in collaboration with the University of Maryland Baltimore County under the NNG11PL02A.

References

[1] Martin D. Johnston et al., Mars Global Surveyor: Aerobraking at Mars, AAS/AIAA Space Flight Mechanics Meeting, Paper 98-112, Monterey, CA, February 2008.

[2] Bruno Victorino Sarli and Yuichi Tsuda, Hayabusa 2 extension plan: Asteroid selection and trajectory design, Acta Astronautica, Volume 138, Pages 225-232, 2017, ISSN 0094-5765, https://doi.org/10.1016/j.actaastro.2017.05.016.

[3] Bruce M. Jakosky et al., The Mars Atmosphere and Volatile Evolution (MAVEN) Mission, Space Science Reviews, Volume 195, Number 1, Pages 3-48, 2015, https://doi.org/10.1007/s11214-015-0139-x.

[4] Alexander S. Konopliv and William L. Sjogren, The JPL Mars gravity field, Mars50c, based upon Viking and Mariner 9 Doppler tracking data, NASA Technical Report, Report Number NASA-CR-198881, JPL-PUBL-95-5, NAS 1.26:198881, February 1995, https://ntrs.nasa.gov/search.jsp?R=19950023923.

[5] H. Justh and V. Keller, Mars Global Reference Atmospheric Model 2005 (Mars-GRAM 2005) User's Guide, December 2005.

[6] The GMAT development team, General Mission Analysis Tool (GMAT) User's Guide R2028a, NASA publication, https://opensource.gsfc.nasa.gov/projects/GMAT/index.php.

[7] Richard H. Battin, An Introduction to the Mathematics and Methods of Astrodynamics, Revised Edition (AIAA Education Series), Pages 450-454, 1999, https://doi.org/10.2514/4.861543.

[8] Katok, A. and Hasselblatt, B., Introduction to the Modern Theory of Dynamical Systems. Cambridge: Cambridge University Press (1995).

[9] Stuart Demcak et al., MAVEN Navigation During the First Mars Year of the Science Mission, AIAA/AAS Astrodynamics Specialist Conference, AIAA SPACE Forum, AIAA 2016-5428, https://doi.org/10.2514/6.2016-5428.

[10] Mark Jesick et al., MAVEN Navigation Overview, 26th AAS/AIAA Space Flight Mechanics Meeting, Paper AAS 16-237, 2016.

[11] Philip E. Gill and Walter Murray and Michael A. Saunders, SNOPT: An SQP algorithm for large-scale constrained optimization, SIAM Review. A Publication of the Society for Industrial and Applied Mathematics, Volume 47, Pages 99-131, 2005, https://doi.org/10.1137/S1052623499350013.